Eur. Phys. J. B **11**, 481–489 (1999)

THE EUROPEAN PHYSICAL JOURNAL B

EDP Sciences

Phase separation and structure in a concentrated colloidal dispersion of uniform plates

A.B.D. Brown[1], C. Ferrero[2], T. Narayanan[2], and A.R. Rennie[3,a]

[1] Semiconductor Physics, Cavendish Laboratory, Madingley Road, Cambridge CB3 0HE, UK
[2] European Synchrotron Radiation Facility, BP 220, 38043 Grenoble Cedex, France
[3] Department of Chemistry, King's College London, Strand, London WC2R 2LS, UK

Received 24 February 1999

Abstract. The structure and phase behaviour of a colloidal dispersion of plate-like particles are described. The plates are nickel (II) hydroxide and have short-range, repulsive interactions and a low polydispersity. As the concentration of the plates is increased, an equilibrium phase separation between a columnar phase and a less ordered phase is observed. Complementary measurements using small-angle neutron and small-angle X-ray scattering have been used to distinguish the columnar phase from other possible ordered structures. Previously isotropic-nematic phase transitions have been observed [1], however this dispersion forms the more highly ordered columnar phase, due to the aspect ratio and the low polydispersity of the plate-like particles. The concentration at which phase separation occurs, increases as the range of the particle interactions is reduced. This system provides an interesting model for comparison with theory and calculations of structures in liquid crystal and mesophase in which the particle interactions can be altered.

PACS. 61.30.Eb Experimental determinations of smectic, nematic, cholesteric, and other structures – 64.70.Md Transitions in liquid crystals

1 Introduction

Dispersions of colloidal particles have been observed to mimic the behaviour of atoms and molecules in certain respects. Monodisperse spheres may, for example, crystallise into highly ordered structures. The arrangement and density of particles in such structures depends on the range of the interactions in relation to the size of the particles. These systems have attracted considerable interest as their larger size (up to a factor of a thousand) gives rise to much slower motion than atomic or molecular materials. Dynamics of phase separation can then be followed using convenient time-scales. It is also possible to tailor systems with particular interactions or mixtures of particle sizes to explore the origin of particular behaviour. Examples of such studies have been work on phase behaviour of mixtures of particles [2], studies of crystallisation of "hard-spheres" and studies of shear induced structures.

Non-spherical, colloidal particles might be expected to display some of the rich phase behaviour of liquid crystals. Indeed dispersions of elongated particles such as vanadium pentoxide which has been described as ribbons [3,4], tobacco mosaic virus (TMV) that forms as rods [5], and more recently boehmite rods [6] have shown equilibrium transitions between isotropic and nematic phases. Dispersions of plate-shaped, gibbsite particles have similarly been observed to display transitions between isotropic and nematic phases [1]. In the nematic phase there is only liquid-like positional order and long range orientational order. Consequently the nematic phase can be and has been observed in systems where the range in particle sizes is quite large. However in order to observe phases with positional order, it is necessary that the particles are sufficiently uniform in size that the ordered phase is not disrupted. This is clearly seen in the case of the crystallisation of spherical particles, where crystallisation of hard spheres is not observed if the range of particle sizes is greater than around 5%.

Large molecules with a plate-like or discotic form are known to form a range of thermotropic, mesophases [7,8]. In some cases columnar phases are observed. At higher temperatures, or on dilution with solvent, less-ordered phases such as a nematic can be found. These systems demonstrate the fine balance in determining the phase behaviour in different systems. Specific interactions generated by dipolar forces and hydrogen bonding can give rise to more complex structures such as cholesteric and twisted phases. It is interesting to explore systems in which ordering will not be dominated by specific inter-molecular forces, to determine the extent to which the shape and density of particles alone can determine the structure.

The repulsive forces between colloidal particles are often considered as being either long-range or short-range

[a] e-mail: rennie@colloids.ch.kcl.ac.uk

forces. Long-range forces arise from charged interactions that can be described by a screened Yukawa potential and short-range forces that arise from the interaction of steric stabilisers adsorbed or grafted to the particle surface. It is possible to control the extent of these forces. The range of the steric forces can be controlled by the molecular length of the stabilisers. The range of the charge interactions are governed by the reciprocal screening length, κ, of an ionic solution containing electrolyte which is given by:

$$\kappa^2 = e^2 \sum n_i z_i^2 / \varepsilon k_B T \quad (1)$$

where e is the electronic charge, n_i the number density of ions of valency z_i, ε the permittivity of the solvent, k_B Boltzmann's constant and T the absolute temperature [9,10]. Addition of salt provides thus an excellent tool for tuning charged interactions. At high concentrations of electrolyte, the repulsive forces are restricted to almost the thickness of the polymer layer providing almost, hard-body interactions for the particles used in the present study.

This paper describes a structural study of concentrated dispersions of plate-like particles at rest and the equilibrium between phases at different concentrations. The work has used dispersions of nickel (II) hydroxide particles that form as hexagonal plates with a range of diameters of ±13%. We have recently reported the observation of a phase that displayed strong positional order [11]. The present work presents a detailed investigation of the structure of the ordered phase observed and the accompanying equilibrium phase transition. Small-angle neutron scattering (SANS) and small-angle X-ray scattering (SAXS) have been used in a complementary manner, allowing the three-dimensional structure of the more ordered phase to be investigated. Papers describing the same system under conditions of continuous shear are currently under preparation.

2 Experimental methods

2.1 Colloidal particles

Plate-like particles of nickel (II) hydroxide were prepared by ageing 0.010 M $Ni(NO_3)_2$ and 0.020 M NH_4OH (reagent grade from Aldrich) at 90 ℃ for two hours, as described by Duran-Keklikian *et al.* [12]. This yielded hexagonal, plate shaped particles as shown in Figure 1. Occasionally particles were observed edge on, such as that ringed in Figure 1, allowing the thickness to be determined as 10 nm. The size distribution of the particles was obtained from measurements of maximum and minimum distances between the opposite flat edges of the particles from micrographs. The results are shown in Figure 2 as histograms. The uniformity of shape as well as size is evident from this data with the average maximum distance between edges being 89 nm ±12 nm and the average minimum distance between the edges being 79 nm ±11 nm.

An independent measure of the particle size was made using small angle X-ray scattering (as described later) from a dilute dispersion of the plates. The scattering (Fig. 3) was fitted with a model for uniform, circular discs [13]. The model assumed the discs were randomly oriented, monodispersed and had no positional order. This gave the radius of the discs to be 90.6 nm and the thickness of the discs as 12.0 nm.

The range of interaction was controlled by adding NaCl to screen the electrostatic forces between the particles. In order to prevent the particles from aggregating when salt was added, a low molecular mass sodium polyacrylate (N40 from Allied Colloids) was added as described previously [11]. The polyelectrolyte dissociated in water so that even with no additional NaCl, up to 0.03 M sodium ions were present. Thus the range of the interactions was governed both by the thickness

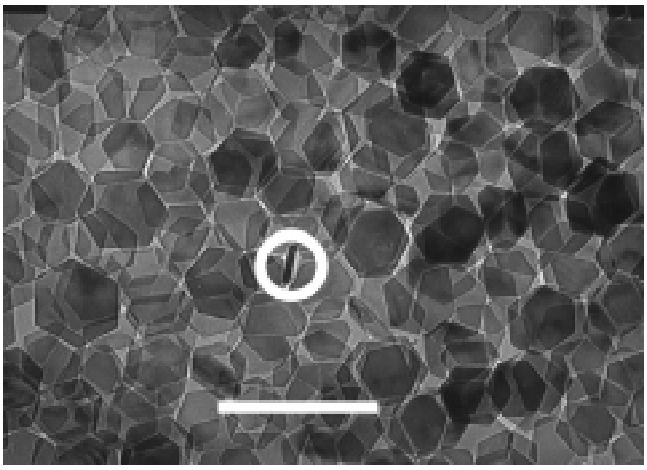

Fig. 1. Transmission electron micrograph of nickel (II) hydroxide particles. The scale bar is 200 nm. The diameter is readily observed, but only rarely (see ring) can edges of the plates be seen. The uncertain tilt makes precise measurement of this dimension difficult.

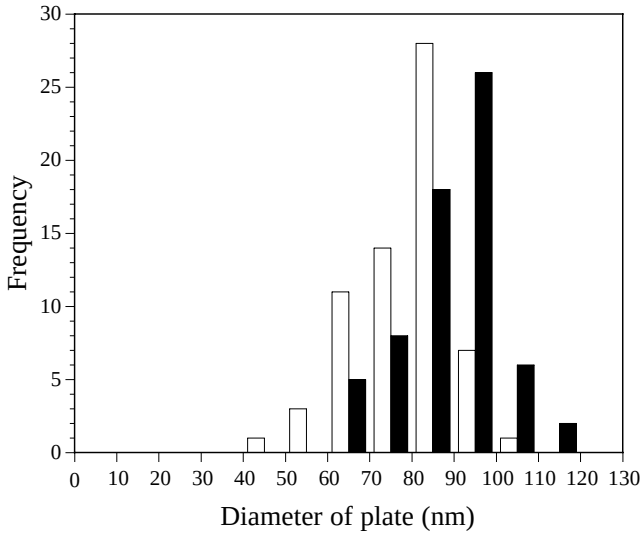

Fig. 2. Histograms of the (■) maximum and (□) minimum edge to edge dimension of each nickel (II) hydroxide plate, observed with a TEM.

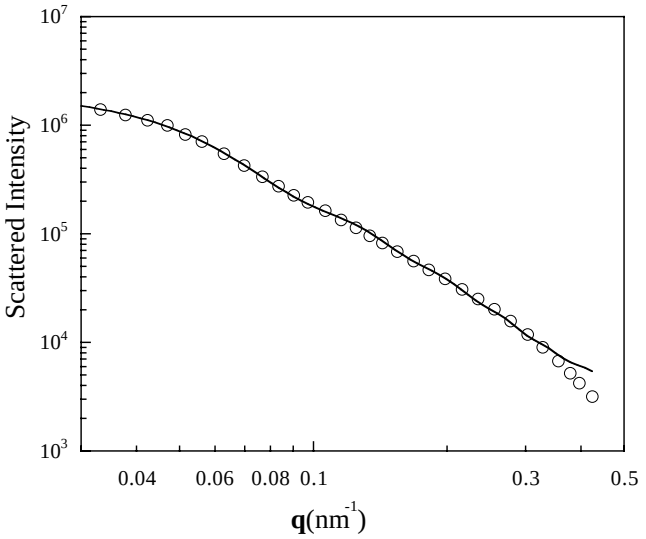

Fig. 3. Radial average of small angle X-ray scattering from a dilute dispersion of the nickel (II) hydroxide plates. The solid line is a curve fit using the predicted scattering for dilute, monodisperse circular plates.

of the polymer layer on the surface of the particles and the range of the electrostatic interactions between the particles.

Measurements were made of the density of a range of dispersions. Combination of this data with measurements of the solid content by drying samples, both with and without adsorbed polyacrylate, to constant weight allows an estimate of the amount of stabiliser attached to the particles. It was calculated that there was 0.114 g of polymer adsorbed per gram of nickel (II) hydroxide. If the polymer layer has a weight fraction of 0.5 and the remainder is water then the thickness of the layer would be 3.5 nm. The thickness of the layer is governed by the length of the polymer chains and their conformation. At 0.03 M Na^+ the screening length for charge interactions is around 3.7 nm. Assuming that the decay of the charge interaction is measured from the centre of the polymer layer, then with no additional salt added the total range of the interactions must lie between 5.4 and 8 nm. If more salt is added then the range of interactions will be reduced for two reasons; the charge interactions between particles will be screened further, and the polymer will have a reduced repulsion with itself, thus reducing the extent it spreads into the solvent. The uncertainty in the thickness of the polymer layer on these particles makes it difficult to provide a precise estimate of the average volume of a particle and thus the volume fractions of the dispersions used. Hence the concentration of dispersions will be described as a weight fraction. The aspect ratio will depend on the thickness of the polymer layer and will be reduced from 8 to between 3.5 and 6 depending upon the concentration of electrolyte and its effect on the polymer. Dynamic light scattering measurements were used to confirm that there was no irreversible aggregation that occurred on preparation of the concentrated dispersions by centrifugation.

2.2 Small-angle scattering

SANS and SAXS techniques were used to investigate the structure of concentrated dispersions. The small-angle neutron scattering experiments were made with the D22 camera on the vertical cold source of the high flux reactor at the Institut Laue-Langevin, Grenoble, France [14]. This apparatus has a 96×96 cm^2 detector with 0.75 cm resolution that can be placed at distances up to 18 m from the sample. The incident beam is monochromated (wavelength, λ) with a mechanical velocity selector giving a spread (FWHM) of 10% $\Delta\lambda/\lambda$. The angular divergence of the incident beam is determined by guides and apertures but the overall resolution in momentum transfer q ($= 4\pi/\lambda \sin(\theta/2)$) results from a combination of the spread in wavelength, angular resolution of the detector elements and the incident beam divergence. In a typical configuration, Δq will vary from about 30% at small momentum transfer to close to 10% at the largest q values. A combination of different sample-detector distances and wavelengths was used to provide data over a q-range from 0.003 to 0.1 Å^{-1}. Samples were contained in fused silica cells with 2 mm path length, the dispersion medium was adjusted to contain about 80% D_2O to reduce the effects of multiple scattering.

The SAXS measurements were made on the ID2 High Brilliance beam line at the ESRF, Grenoble, France [15]. This instrument is equipped with a silicon double monochromator and focussing mirror which provide high monochromaticity $\Delta\lambda/\lambda$ (FWHM) 0.02% and a low divergence. The angular divergence is less than 0.001 5 degrees vertically and 0.002 5 degrees horizontally. Beam size was defined by apertures and was 0.2 mm (vertical) by 0.36 mm (horizontal). A gas filled two-dimensional detector with 0.5 mm spatial resolution was used at a distance of 10 m from the sample. The width of diffraction peaks is effectively limited by the point spread function of the detector (0.6 mm).

Small-angle neutron scattering allowed samples with a thickness of 2 mm to be investigated so that the effect of the cell surfaces was small. In contrast, X-rays have a higher absorption and scattering. Only thin samples could be investigated, however the X-ray source at the ESRF provides an intense beam that can be highly monochromated and collimated. This meant that the width of any SAXS peaks were determined by the sample and not the instrument. The high intensity of the beam also meant that a small area of the sample could be investigated to probe areas showing uniform alignment. Samples for SAXS studies were placed in 0.4 mm thick flat-sided thin-walled glass tubes aligned on a goniometer head allowing rotation about a vertical axis.

In both the case of SANS and SAXS data was treated with standard programs to account for relative efficiency of detector cell and subtract the background. The X-ray data was corrected for detector efficiency, flat-field response and background from the instrument and cell. The conversion to absolute intensity was made by measurement of transmitted flux and the intensity from a Lupolen standard sample. Data was inspected as two-dimensional

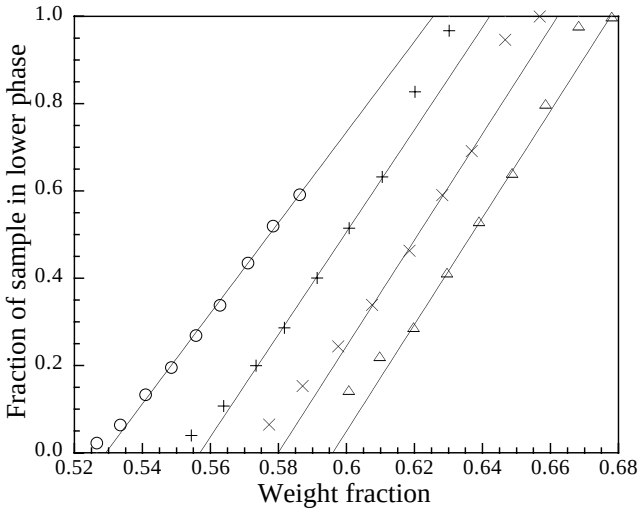

Fig. 4. Fraction of the cell occupied by the more dense, ordered phase for a series of samples with different, overall weight fractions at three different salt concentrations after 36 days. (○) 0 M, (+) 0.02 M, (×) 0.05 M, and (△) 0.1 M NaCl added.

Table 1. Weight fractions of the two phases that are in equilibrium at the four concentrations of added salt investigated.

Added NaCl (M)	Upper phase (wt. fraction)	Lower phase (wt. fraction)	Difference between two phases (wt. fraction)
0	0.529	0.625	0.096
0.02	0.557	0.642	0.085
0.05	0.580	0.662	0.082
0.1	0.596	0.678	0.082

images and also converted to circular averages of intensity as function of momentum transfer, either for the entire detector or in individual sectors at particular orientations. In this way data from different instrument configurations could easily be combined and compared. Crystallography of large-scale structures measured by low-angle diffraction presents some unusual features [16]. The ratio of spacing to wavelength is large and only a small part of the Ewald sphere is accessible. It can be difficult to determine intensities of Bragg reflections for peaks other than those lying in one plane. Distinction between 3-dimensional structure with spots and cuts through patterns of lower order with rods or sheets of intensity in the scattering pattern can sometimes be difficult.

3 Results

3.1 Visible phase separation

For all the concentrations of added electrolyte considered, it was found that there was a range of particle concentrations over which droplets formed in the bulk of the dispersion. These droplets then sedimented over a number of days, and formed a dense lower phase with a more dilute upper phase. This could be observed readily, and the droplets and the resulting lower phase displayed some birefringence, whereas no birefringence was observed in the upper phase. The fraction occupied by the more dense phase for samples with 0 M, 0.02 M, 0.05 M and 0.1 M added NaCl are shown in Figure 4, plotted against the total weight fraction of the sample. Over most of the region where two phases are present, the volume of the concentrated phase varies linearly with weight fraction, indicating the phase separation is true equilibrium coexistence. There is a small deviation from this linear behaviour at high weight fractions, as the viscosity of the sample at these concentrations slowed the phase separation. At low weight fractions there is also a deviation, as at this concentration the viscosity was much lower, and so sedimentation of the particles (as opposed to droplets of the denser phase) was measurable, causing an increase in the volume of the lower phase. The weight fractions of the two phases in equilibrium are given in Table 1. The phase separation is observed at increasing particle concentrations with increasing electrolyte concentration due to the shorter range of the inter-particle forces. The difference between the two equilibrium concentrations decreases slightly as the range of the particle interactions is reduced.

The lower phase appeared to be an agglomeration of droplets with a diameter of around 40 μm. More detailed optical observations could not be made as samples greater than 1 mm in thickness were opaque due to the strong green colour of the sample. If the samples were placed in thinner tubes, the droplets tended to stick to the surface of the glass and were consequently distorted.

3.2 Neutron scattering patterns

A number of dispersions at a wide range of weight fractions were investigated by small-angle neutron scattering. The radial average of the scattering patterns obtained from these samples over a wide range of q are shown in Figure 5. Sample A, at a concentration above the phase separation region and sample B, within the phase separation regime both display a series of diffraction peaks. The peaks can be indexed on the basis of a crystallographic hexagonal cell with $a = b$, $\gamma = 120$ degrees. The positions, corresponding d-spacings and Bragg indices of these peaks are given in Table 2. The peaks in sample A are at slightly larger q than in sample B, suggesting that the structure is slightly compressed above the phase separation regime. The way in which these peaks are indexed will be discussed later in this paper. Sample A was sufficiently viscous that it could only be inserted in the cell by gentle centrifugation. As a consequence the two-dimensional scattering patterns shown in Figure 6a and b indicate a preferential orientation of peaks 100 and 001 showing that they arise from orthogonal directions within the sample. To show the preferential alignment, the data is show with a threshold around the maximum intensity in each of the two ranges of momentum transfer measured.

Table 2. Concentrations of dispersions of nickel (II) hydroxide investigated with SANS.

Sample	Weight fraction (±0.003)	Added salt concentration (M)	Comment
A	0.677	0.040	above phase separation
B	0.614	0.040	48% upper separated region
C	0.566	0.040	just below phase separation
D	0.365	0.030	much below phase separation
E	0.02	0.030	dilute

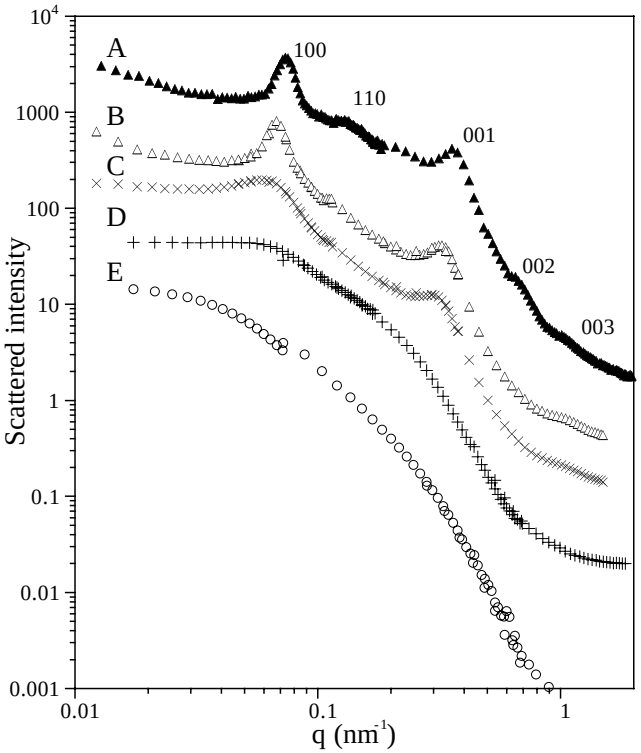

Fig. 5. The scattered intensity from sample A, B, C, D and E. Details of the samples are given in Table 2. For clarity each data set has been offset vertically.

3.3 Small-angle X-ray scattering patterns

A sample above the phase separation regime was placed in a flat cell, 0.4 mm thick, for the measurements. The scattering pattern from the sample with the beam perpendicular to the flat face of the tube is shown in Figure 7a. The pattern very clearly shows hexagonal order within the sample indicating that inserting the sample in the cell must have orientated it to almost a perfect crystal. The scattering from the same point in the sample when it is turned by 20 degrees about a vertical axis is displayed in Figure 7b. This shows how some of the peaks disappear as the sample is turned, the radial average of the pattern in Figure 7a is shown in Figure 8. The position of the peaks in these plots is very similar to those observed with neutron diffraction from sample A. This indicates that the structure is not significantly altered by the size of the cell that the sample is placed in.

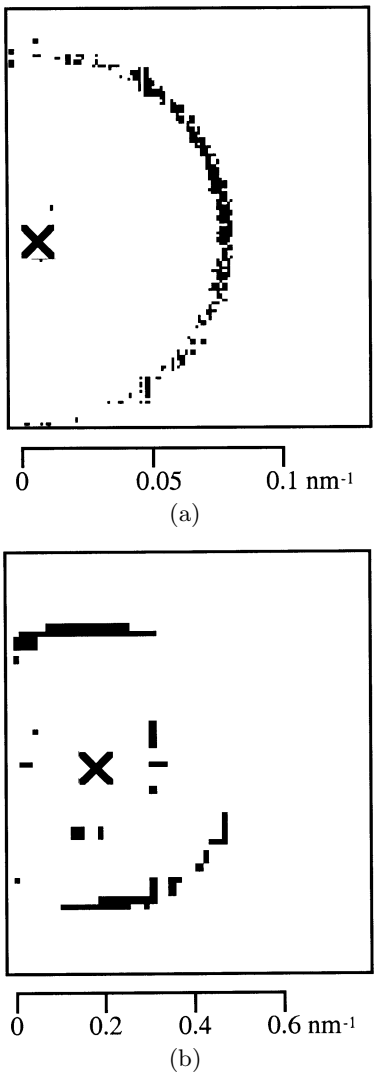

Fig. 6. SANS patterns from sample A, (a) 100 peak, (b) 001 peak. A threshold has been used to reveal the slight anisotropy present in the two primary diffraction rings. The X marks the position of the unscattered beam.

4 Discussion

4.1 Distinguishing possible structures

The positions of the 001, 002 and 003 peaks observed with SANS from sample A are consistent with their being first,

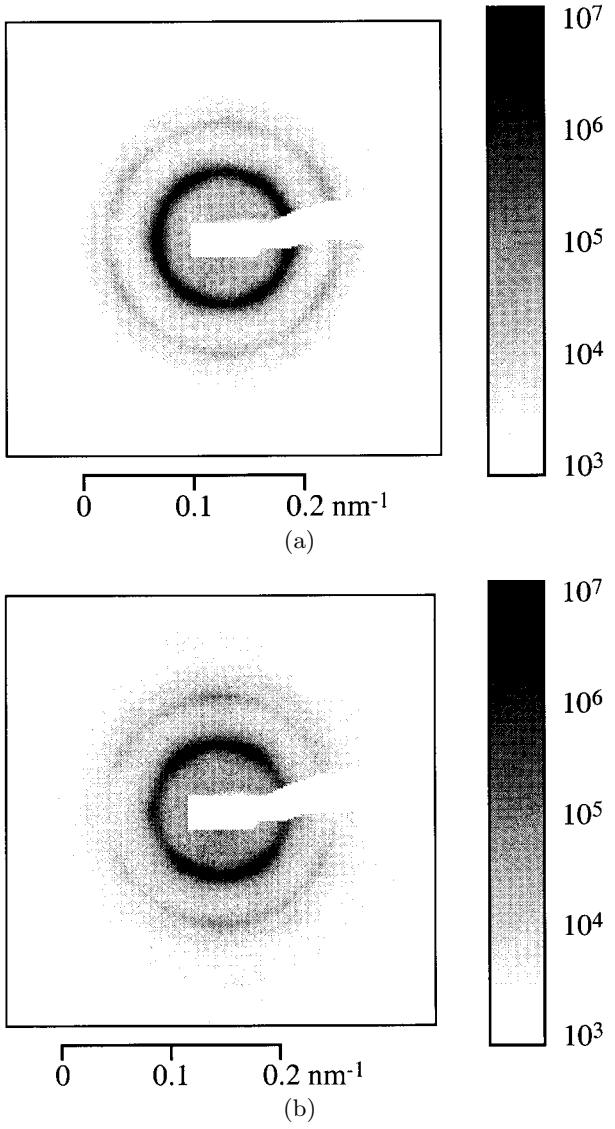

Fig. 7. SAXS pattern from a sample above the phase transition regime, in a flat cell mounted (a) perpendicular to the beam, (b) rotated by 20 degrees about a vertical axis.

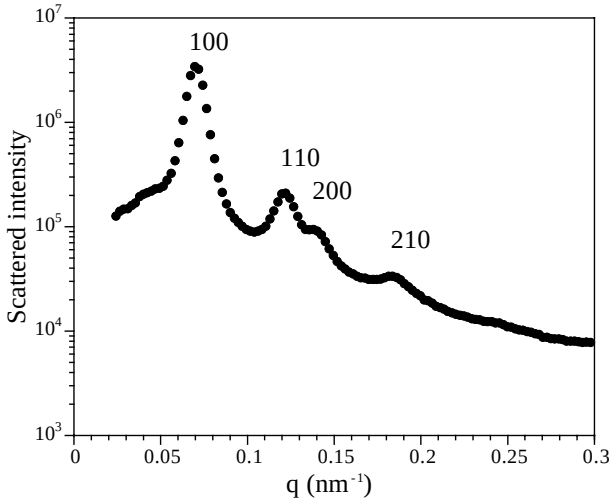

Fig. 8. Radial average of the SAXS pattern shown in Figure 7a.

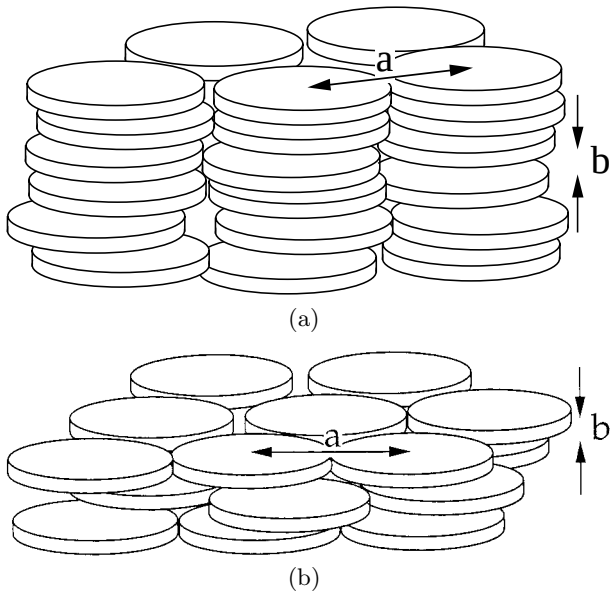

Fig. 9. Two possible schematic structures of the dense, more ordered phase. (a) a columnar structure, (b) a layer structure. Distance a is related to peak 100 and distance b is related to peak 001.

second and third orders of a single d-spacing associated with a length scale of the order of the thickness of the plates. This distance puts a limit on the thickness of the polymer layer. The thickness of the nickel (II) hydroxide crystal is 10 nm and the distance corresponding to the 001 peak from sample A is 20 nm. Thus if the polymer layer is not highly compressed in sample A, it cannot be greatly thicker than 5 nm. The position of the 100 peak suggests that it is associated with a feature of the order of the diameter of the particles. This is consistent with the observation made from the anisotropy in Figure 6. The pattern observed with the SAXS measurements shown in Figure 7a suggests that the packing in the plane perpendicular to the plate normals is hexagonal. The second peak that can just be observed in the SANS measurements is consistent with being the 110 and the 200 peaks from hexagonal packing, which are not resolved with SANS due to the instrument resolution, but are resolved in Figures 7 and 8 with SAXS. The peak positions observed in these diffraction patterns from the ordered phase could result from two types of structures that are sketched in Figure 9. In a columnar structure (Fig. 9a), the 001, 002 and 003 peaks would correspond to a regular spacing of particles along columns, stacked face-to-face. The 100, 110 and 200 peaks would arise from the hexagonal packing of the columns. In this structure there need not be any correlation between positions of particles in different columns. In a layer structure such as that in Figure 9b, the 100, 110 and 200 peaks would

correspond to scattering from within layers of hexagonally arranged particles. The 001, 002 and 003 peaks would then correspond to the stacking of these layers at a regular spacing, but no lateral correlation of adjacent layers would be required. A third possibility would be a crystalline combination of these two structures where there is no loss of correlation between the layers or columns of particles.

These two structures are represented in different ways in reciprocal space [17]. The columnar structure would be represented by layers normal to the real space columns, except for the layer containing the origin that breaks up into spots corresponding to the relative positions of the columns. The layer structure would be represented by rods normal to the sheets of particles, except for the rod containing the origin, which breaks up into spots corresponding to the spacing between the layers.

If a single crystal was placed in a range of different orientations in the beam, all directions of reciprocal space could be investigated. This would allow the structure of the crystal to be determined. Alternatively it would also be possible to distinguish between the possible structures from the peak shapes and intensities of the scattering from a powder with a known preferred orientation.

The samples investigated with SANS were partially orientated powders due to the influence of the walls and some shear-induced order as the sample was inserted into the cell. However the extent of orientation was not known. This meant the intensities were altered by the partial orientation of the domains, making it impossible to use the intensity information in this data to distinguish between the proposed crystal structures [11]. The width and hence the shape of the peaks were dominated by the instrument resolution, and so also could not be used to determine the crystal structure.

The sample investigated with SAXS was a strongly orientated powder and so can be considered as an approximation to a single crystal. A region showing particularly strong alignment was selected for study by scanning the position of the sample with respect to the incident beam. Figure 7a is the plane in reciprocal space that contains the origin and whose normal is parallel to the plate normals. If the particles were in layers with normals parallel to the plate normals (Fig. 9b), then the lack of positional correlation between particles in different planes would mean the spots seen in Figure 7a would be cuts through rods perpendicular to the page. If all the particles were correlated in this direction, such as in both the columnar structure and a three dimensional crystal, then the spots observed in Figure 7a would be cuts through short arcs around the origin due to the range of domain orientations. To determine which is the case, the sample was rotated about a vertical axis by 20 degrees and the pattern obtained is shown in Figure 7b. If the spots observed in Figure 7a were cuts through rods, then in the cut through reciprocal space shown in Figure 7b they should appear as spots, shifted horizontally to larger q. This is not the case. The spots remain at the same magnitude of q, indicating that the scattering observed is a cut through an arc. Thus the structure cannot be formed of layers but must be either columnar or crystalline.

In theory the same approach could be used to investigate whether there is positional correlation between particles in different columns. However the sample was in a flat tube and so it was not possible to investigate the direction perpendicular to the tube, as this would require the beam to be incident in the plane of the tube.

It can be concluded from these X-ray measurements that the particles must be in columns (Fig. 9a), as they cannot be in uncorrelated layers, and the hexagonal packing shows no absences. However from these measurements it is not possible to say the extent of any positional correlation between these columns.

4.2 Dilute phase

The dilute phase displays no birefringence, and so cannot be a nematic phase. Samples C, D, and E are all below the point of phase separation; however the scattering observed from them, shown in Figure 4, shows a range of structure present. Sample E is at a weight fraction of 0.02 and so will be at a volume fraction of approximately 0.006. At this concentration there will be very little interaction between the particles, and so the scattering will be essentially the spherical average of the form factor of the particles. The scattering profile from sample D is a different shape. This is due to interactions between the particles, giving them some kind of liquid positional order. Sample C that is just below the phase separation regime displays significantly more order. This increase in order between samples D and C could be a progressive increase in liquid order, or it could be due to a further phase transition from an isotropic structure in sample D to a more ordered structure in sample C. No phase separation was observed at any concentration investigated between that of sample C and D. However, a more detailed scattering study would be required to determine if a phase transition exists in this region.

4.3 Comparison with simulation and other systems

Results from computer simulations on dispersions of platelike particles and their phase transitions are reported in the literature [18]. A sketch of the expected phase diagram is shown in Figure 10. It is predicted that for discs with an aspect ratio of 5 and hard interactions, as concentration is increased, a first order transition from an isotropic phase to a cubatic phase occurs between $\rho^* = 0.54$ and 0.57. There is then a first order transition to a columnar phase with phase separation between $\rho^* = 0.59$ and $\rho^* = 0.66$, and finally a continuous transition to a solid at $\rho^* = 0.73$. ρ^* is defined as being the ratio of the volume fraction to that of a close packed structure. The observations made here are consistent with these predictions on a number of points. A nematic phase is not observed and a first order transition to a columnar phase is observed

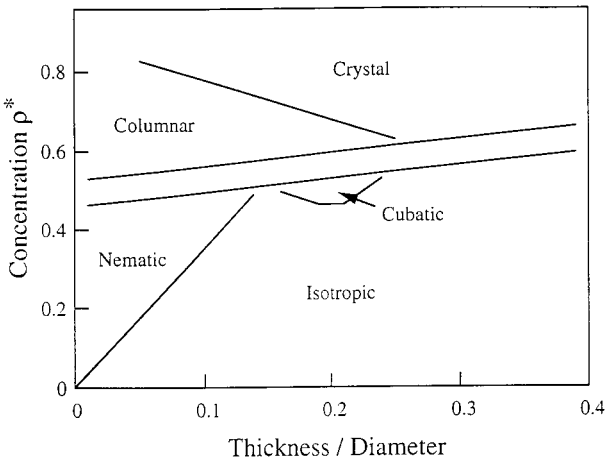

Fig. 10. Phase diagram for plate-like particles that has been suggested by computer simulation of Veerman and Frenkel [18].

with a phase separation between dispersions at a concentration of $\rho^* = 0.393$ and $\rho^* = 0.498$ for a polymer layer thickness of 3.5 nm and $\rho^* = 0.605$ and $\rho^* = 0.766$ for a coat thickness of 8 nm. Our present data has not allowed us to determine the structure of the less concentrated phase that may not be an isotropic liquid.

The observed difference in concentration between the coexistent phases is twice that predicted in the simulations. This separation in concentration of the two coexisting phases is termed the biphasic gap by Bates and Frenkel [19]. The unusually large region could be caused by the presence of attractive forces between the particles. However the gap was observed to decrease slightly as salt is added. This suggests that significant attractive forces are not present, as it would be expected that the effect of any attractive forces would enhanced as the repulsive electrostatic forces are screened by adding salt, and this should increase the biphasic gap. An alternative explanation for this large biphasic gap arises from the simulations of Bates and Frenkel [19]. They studied the nematic-isotropic transition as a function of the polydispersity in the diameter of infinitely thin plates. They found that 14% polydispersity approximately doubles the biphasic gap. By analogy it might well be expected that the polydispersity present in the system studied here (13% in the diameter) could well account of the large biphasic gap observed.

In their original simulations Veerman and Frenkel [18] predict that samples with concentrations in the region of C should form a cubatic phase. This phase is described as a structure in which the particles assemble in short stacks of approximately 4 or 5 particles with neighbouring stacks tending to be approximately perpendicular. There is no long-range positional order. This phase would be expected to have a peak in the 001 position arising from spacings between the faces of the plates. The short stacks would mean that this peak should be broader and less intense than the peaks observed in the columnar phase. There would also be a weak peak in the 100 position arising from the spacing between the short stacks in the dispersion. These differences would depend on the degree of positional correlation in each structure and so are not straight forward to interpret. The scattering observed from sample C shows these features; however a phase transition between sample C and D would need to be observed before a definite statement could be made.

There are some differences between these results and those observed for gibbsite [1] where there is clear evidence of a wider range of stability for a nematic phase. There are several differences between that material and the nickel hydroxide plates. The polydispersity in particle size may be crucial. Bates and Frenkel have simulated thin, polydisperse plates and suggested that this gives rise to size segregation [19]. Bates has also investigated the effect of shape [20] and has shown that exclude volume can be used to scale the behaviour but both gibbsite and nickel hydroxide form substantially hexagonal particles.

The observation that the phase boundary (Fig. 4) moves to higher concentrations as the salt concentration increases, is expected as the particles interact over a shorter distance. The difference in concentration of the two phases in equilibrium decreases. It is not clear whether this might be attributed to a change in the effective aspect ratio of the particles or simply to the range of the interactions between the particles. This would be an interesting study for further experimental, theoretical, and computer studies.

5 Conclusions

A dispersion of plate shaped particles with a small range of particle sizes and shapes has been studied. The plates have an aspect ratio of 3.5–6 and a range of interaction less than 10% of the particle diameter. As the concentration of such plates is increased, an equilibrium phase transition to a columnar structure is observed. Reducing the range of particle interactions increases the concentration at which the phase transition occurs, and reduces the range of concentrations over which phase co-existence is observed. Although other work has reported an isotropic to nematic phase transition in a dispersion of plate-like particles [1] this observation of a columnar phase is new. The high monodispersity and the particular aspect ratio of the stabilised $Ni(OH)_2$ particles gives rise to this structure. This system provides a test for computer simulations such as those of Veerman and Frenkel [18]. The combination of small-angle scattering on aligned samples with direct optical observation of phase separation provides a valuable tool to investigate model mesophase materials.

We are grateful for discussions with Felix van der Kooij about his work and to Daan Frenkel and Martin Bates for sending us pre-prints of their work. We thank the ILL and ESRF for beam time. ABDB thanks the UK EPSRC for a research studentship.

References

1. F.M. van der Kooij, H.N.W. Lekkerkerker, J. Phys. Chem. B **102**, 7829 (1998).
2. M.D. Eldridge, P.A. Madden, P.N. Pusey, P. Bartlett, Molecular Phys. **84**, 395 (1995).
3. H. Zocher, Z. Anorg. Chem. **147**, 91 (1925).
4. P. Davidson *et al.*, J. Phys. II France **5**, 1577 (1995).
5. J.D. Bernal, I. Frankuchen, J. Gen. Physiol. **25**, 111 (1941).
6. M.P.B. van Bruggen, F.M. van der Kooij, H.N.W. Lekkerkerker, J. Phys-Cond. Matter **8**, 9451 (1996).
7. S. Chandrasekhar, *Liquid Crystals*, 2nd edn (Cambridge University Press, Cambridge 1992).
8. P.G. de Gennes, J. Prost, *The Physics of Liquid Crystals*, 2nd edn (Oxford University Press, Oxford 1993).
9. D.H. Everett, *Basic Principles of Colloid Science* (Royal Society of Chemistry, London, 1992).
10. R.J. Hunter, *Foundations of Colloid Science: I* (Oxford University Press, London, 1992).
11. A.B.D. Brown, S.M. Clarke, A.R. Rennie, Langmuir **14**, 3129 (1998).
12. L. Durand-Keklikian, I. Haq, E. Matijevic, Colloids and Surf. A: Physicochem. Eng. Aspects **92**, 267 (1994).
13. H.C. van de Hulst, *Light Scattering by Small Particles* (Chapman and Hall Ltd., London 1957).
14. H.G. Büttner, E. Lelièvre-Berna, F. Pinet, *Guide to Neutron Scattering Facilities at the ILL* (ILL Grenoble 1997).
15. P. Boesecke, O. Diat, B. Rasmussen, Rev. Sci. Inst. **66**, 1636 (1995).
16. S.M. Clarke, A.R. Rennie, R. H. Ottewill, Langmuir **13**, 1964-1969 (1997).
17. A. Guinier, *X-Ray Diffraction in Crystals, Imperfect Crystals and Amorphous Bodies* (W.H. Freeman and Company, San Francisco, 1963).
18. J.A.C. Veerman, D. Frenkel, Phys. Rev. A **45**, 5632 (1992).
19. M.A. Bates, D. Frenkel, J. Chem. Phys. **110**, 6553 (1999).
20. M.A. Bates (in preparation, 1999).